

Original article

A comparative study of the hydrolysis pathways of substituted aryl phosphoramidate versus aryl thiophosphoramidate derivatives of stavudine

T.K. Venkatachalam ^{a,*}, G. Yu ^a, P. Samuel ^b, S. Qazi ^c, S. Pendergrass ^d, F.M. Uckun ^d

^a Department of Chemistry, Parker Hughes Institute, 2699 Patton Road, Roseville, MN 55113, USA

^b Department of Pharmaceutical Sciences, Parker Hughes Institute, 2699 Patton Road, Roseville, MN 55113, USA

^c Department of Bioinformatics, Parker Hughes Institute, 2699 Patton Road, Roseville, MN 55113, USA

^d Departments of Virology and Immunology, Parker Hughes Institute, 2699 Patton Road, Roseville, MN 55113, USA

Received 5 December 2003; received in revised form 28 April 2004; accepted 28 April 2004

Abstract

A comparative study of aryl phosphoramidate and aryl thiophosphoramidate derivatives of 2',3'-didehydro-2',3'-dideoxythymidine (d4T) was performed. The study focused on the nature of the substituents and the influence of a thiophosphoramidate in the structure of these derivatives. The rate of alkaline hydrolysis of these two types of d4T derivatives indicated that replacement of oxygen with sulfur decreases the rate of hydrolysis by twofold. Additionally, the activation energy (E_a) for the sulfur analogs is comparatively higher than that of the oxygen analogs. Notably, an intermediate was formed in the hydrolysis reaction of the sulfur analogs of d4T that was absent in the case of the oxygen analog, and the tentative structure of the intermediate was proposed based on LC/mass spectroscopy data. Using both HPLC and ³¹P-NMR techniques, we identified the hydrolysis product of the phosphoramidate derivatives and were able to show in *in vitro* studies that porcine liver esterase can hydrolyze the methyl ester portion of the phosphoramidate derivatives. Aryl phosphoramidate derivatives of d4T were 1000-fold more active than the corresponding aryl thiophosphoramidate derivatives, indicating that the energy of activation of hydrolysis of these phosphoramidate derivatives plays a significant role in their biological potency.

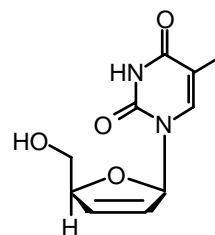
© 2004 Elsevier SAS. All rights reserved.

Keywords: Phosphoramides; Thiophosphoramides; Stavudine; Activation energy; HPLC; ³¹P-NMR

1. Introduction

Acquired immunodeficiency syndrome (AIDS) is the disease affecting a significant part of the population in recent years due to the epidemic spread of human immunodeficiency virus (HIV) [1–7]. Three categories of anti-retroviral agents in clinical use are nucleoside analogs, nucleoside reverse transcriptase inhibitors (NRTI), such as zidovudine and stavudine 2',3'-didehydro-2',3'-dideoxythymidine (d4T, **1**), protease inhibitors and non-nucleoside reverse transcriptase inhibitors (NNRTI) [4–7]. The 5'-triphosphates of 2',3'-dideoxynucleoside analogs (ddN) that are generated by nucleoside and nucleotide kinases, are potent inhibitors of HIV reverse transcriptase [8–9]. The rate limiting step for the conversion of 3'-azido-3'-deoxythymidine (AZT) to its bio-

active metabolite, AZT-triphosphate, seems to be the conversion of the monophosphate derivative to the diphosphate derivative, whereas the rate limiting step for the intracellular generation of the bioactive metabolite of **1**, stavudine-triphosphate, was reported to be the conversion of the nucleoside to its monophosphate derivative [10–12]. Anti-HIV ddN derivatives primarily rely on nucleoside and nucleotide kinases to convert them into the corresponding 5'-



1

* Corresponding author.

E-mail address: jhumphrey@ih.org (T.K. Venkatachalam).

triphosphates as discussed before. However, such compounds were found to act as poor substrates for nucleoside kinases [10,13–16]. Consequently, development of pro-drug strategies were sought that could bypass the initial nucleoside kinase activation. In an attempt to overcome the dependence of ddN analogs on intracellular nucleoside kinase activation, we and others have prepared aryl phosphate derivatives of zidovudine and **1** [11,12,17–21]. Some of these derivatives were found to be potent anti-HIV agents with subnanomolar IC₅₀ values. In the present study, we prepared thiophosphoramidate derivatives of **1** and compared their alkaline hydrolysis rates with those of phosphoramidate derivatives.

2. Chemistry

NMR spectra were obtained at ambient temperature in deuterated solvent. Chemical shifts are reported as δ values in parts per million and referenced to the solvent or an internal standard. Coupling constants (J) are reported in Hz. FT-IR spectra were obtained as KBr pellets. Melting points (m.p.) are uncorrected. HPLCs were obtained using an analytical RP-18 Lichrospher column, 5 μ m (4.6 \times 150 μ m) and acetonitrile/water as the eluent. The flow rate was maintained at 1.0 ml min⁻¹ and the detection wavelength was set at 266 nm. The column was maintained at room temperature throughout the analysis. Column and TLC chromatography was performed using silica gel 60, 230–400 mesh. Compounds **7–12** were prepared according to previously published methods [6].

Typical procedure for the preparation of aryl thiophosphoramidate derivatives of 1,2',3'-didehydro-3'-deoxythymidine 5'-(*p*-bromophenyl methoxyalaninyl thiophosphate) (**4**). Under a nitrogen atmosphere, a solution of *p*-bromophenol (34.60 g, 0.20 mol) and triethylamine (27.85 ml, 0.20 mol) in anhydrous diethyl ether (200 ml) was added dropwise to a vigorously stirred solution of thiophosphoryl chloride (20.31 ml, 0.20 mol) in ether (300 ml) at 0 °C. The mixture was allowed to warm to ambient temperature, with stirring for 5 h, and then heated under reflux for 2 h. The mixture was filtered and the precipitate was washed with diethyl ether (100 ml). The combined filtrate and washings were evaporated to dryness under reduced pressure to yield colored oil. The oil was subjected to vacuum distillation to yield the product as a colorless oil (*p*-bromoarylthiophosphorylchloride). Yield: 50%; b.p.: 140–143 °C/0.7 mm [6]. A solution of L-alanine methyl ester hydrochloride (0.28 g, 2.0 mmol) and 1.0 ml triethylamine in anhydrous acetonitrile (20 ml) was added dropwise with vigorous stirring to a solution of 2.0 mmol of appropriately substituted aryl thiophosphoryl chloride in 20 ml anhydrous acetonitrile at 0 °C. The reaction mixture was slowly warmed to ambient temperature with stirring, and 0.35 g (5.0 mmol) of 1,2,4-triazole was added to the reaction mixture. The contents were stirred at room temperature for 6 h, and 0.224 g (1.0 mmol) of d4T was added and the reaction was allowed to stir at 50 °C for

2 weeks. Solvent was evaporated under reduced pressure to furnish viscous oil. The crude reaction product was further purified using column chromatography using (chloroform/methanol = 10:1). The appropriate fractions were pooled together and once again the solvent was removed under reduced pressure to yield a viscous oil which was subsequently subjected to preparative TLC (chloroform/methanol) = 10:1 to obtain analytically pure compound in 12.3% yield. Further modifications of this procedure using solvents such as dichloromethane, chloroform and carrying out the reaction at room temperature did not yield the desired product. An increase in temperature beyond 50 °C resulted in decomposition of the product.

2.1. 2',3'-Didehydro-3'-deoxythymidine 5'-(4-bromo-phenyl methoxyalaninyl thiophosphate) (**4**)

¹H-NMR (300 MHz, CDCl₃) δ 1.37 (m, 3H), 1.81 (s, 3H), 3.73 (d, 3H, J = 5.1 Hz), 4.02–4.41 (m, 4H), 5.04 (m, 1H), 5.92 (s, 1H), 6.32 (m, 1H), 6.99–7.10 (m, 3H), 7.26 (m, 1H), 7.43 (d, 2H, J = 8.4 Hz), 8.62 (m, 1H). ¹³C-NMR (75 MHz, CDCl₃) δ 12.8, 21.3, 51.2, 53.0, 67.2, 68.1, 84.7, 90.1, 111.5, 118.7, 123.1, 127.6, 132.7, 133.6, 135.8, 149.6, 150.8, 163.6. ³¹P-NMR (121 MHz, CDCl₃) δ -14.39, -13.92. UV (MeOH) λ_{max} : 224 (sh), 265 nm. IR (KBr, cm⁻¹): 3456, 2360, 1693, 1483, 1216, 1143, 1011, 912, 828. HPLC: 19.3, 19.7 min.

2.2. 2',3'-Didehydro-3'-deoxythymidine 5'-(phenyl methoxyalaninyl thiophosphate) (**2**)

¹H-NMR (300 MHz, CDCl₃) δ 1.37 (m, 3H), 1.80 (s, 3H), 3.73 (d, 3H, J = 6.6 Hz), 3.96–4.44 (m, 4H), 5.04 (m, 1H), 5.90 (s, 1H), 6.33 (m, 1H), 6.83 (d, 2H, J = 8.7 Hz), 7.02 (m, 1H), 7.12–7.34 (m, 6H), 8.36 (m, 1H). ¹³C-NMR (75 MHz, CDCl₃) δ 12.6, 21.4, 51.1, 53.0, 67.0, 67.9, 84.9, 90.1, 111.6, 121.2, 125.6, 127.4, 129.7, 133.6, 135.9, 150.7, 163.6. ³¹P-NMR (121 MHz, CDCl₃) δ -14.64, -14.24. UV (MeOH) λ_{max} : 265 nm. IR (cm⁻¹): 3297, 1693, 1593, 1489, 1211, 1149, 1091, 923, 776, 756. LC/MS: 511 (M + Na). HPLC: 16.1, 16.5 min. Yield: 11.7%.

2.3. 2',3'-Didehydro-3'-deoxythymidine 5'-(*p*-fluorophenyl methoxyalaninyl thiophosphate) (**3**)

¹H-NMR (300 MHz, CDCl₃) δ 1.37 (m, 3H), 1.82 (s, 3H), 3.73 (d, 3H, J = 4.8 Hz), 3.96–4.42 (m, 4H), 5.04 (m, 1H), 5.93 (s, 1H), 6.33 (m, 1H), 7.01–7.32 (m, 6H), 8.30 (m, 1H). ¹³C-NMR (75 MHz, CDCl₃) δ 12.7, 21.4, 51.2, 53.0, 67.1, 68.0, 84.8, 90.1, 111.5, 116.4, 122.7, 127.5, 133.5, 135.8, 150.7, 163.5. ³¹P-NMR (121 MHz, CDCl₃) δ -13.56, -13.88. ¹⁹F-NMR (282 MHz, CDCl₃) δ -41.57. UV (MeOH) λ_{max} : 265 nm. IR (cm⁻¹): 3261, 1693, 1509, 1457, 1196, 1149, 1089, 916, 839. LC/MS: 522 (M + Na). HPLC: 17.0, 17.3 min. Yield: 8.3%.

2.4. 2',3'-Didehydro-3'-deoxythymidine 5'-(p-methoxyphenyl methoxyalaninyl thiophosphate) (5)

$^1\text{H-NMR}$ (300 MHz, CDCl_3) δ 1.40 (m, 3H), 1.82 (s, 3H), 3.73 (d, 3H, $J = 5.4$ Hz), 3.78 (m, 3H), 3.88–4.42 (m, 4H), 5.03 (m, 1H), 5.90 (s, 1H), 6.33 (m, 1H), 6.83 (d, 2H, $J = 8.7$ Hz), 6.99 (m, 1H), 7.04–7.11 (m, 2H), 7.29 (m, 1H), 8.18 (m, 1H). $^{13}\text{C-NMR}$ (75 MHz, CDCl_3) δ 12.9, 21.4, 51.1, 53.0, 55.9, 67.0, 67.9, 84.9, 90.0, 111.6, 114.7, 122.1, 127.4, 133.6, 135.9, 144.0, 150.7, 157.1, 163.5. $^{31}\text{P-NMR}$ (121 MHz, CDCl_3) δ -13.69, -13.27. UV (MeOH) λ_{max} : 225 (sh), 270 nm; IR (cm^{-1}): 3287, 2953, 1690, 1506, 1466, 1201, 1145, 1034, 912. LC/MS: 542 (M + Na). HPLC: 16.2, 16.4 min. Yield: 16.1%.

2.5. 5'-[4-Fluorophenyl methoxyalaninyl phosphate]-2',3'-didehydro-3'-deoxy thymidine (9)

Yield: 46%, m.p. 42–44 °C, UV (MeOH) λ_{max} : 210 and 266 nm; IR: 3423, 3245, 3072, 2954, 1691, 1504, 1247, 1089, 1037, 939 cm^{-1} . $^1\text{H-NMR}$ (CDCl_3) δ 10.08 (bs, 1H), 7.16 (m, 1H), 7.08 (m, 2H), 6.91 (m, 3H), 6.20 (m, 1H), 5.79 (t, 1H), 4.92 (m, 1H), 4.42 (t, 1H), 4.22 (m, 2H), 3.85 (m, 1H), 3.58* (m, 3H), 1.70* (m, 3H), 1.22* (m, 3H); $^{13}\text{C-NMR}$ (CDCl_3) δ 173.5 (q), 163.8 (d), 160.7, 157.5, 150.7 (d), 145.7 (q), 135.3 (d), 132.7 (d), 126.9 (d), 121.3 (t), 115.8 (q), 110.8 (d), 89.2 (d), 84.2 (d), 66.8 (t), 52.2, 49.8 (d), 20.4 (d), 12.1 (d); $^{31}\text{P-NMR}$ (CDCl_3) δ 3.80 (d), 3.22 (d); $^{19}\text{F-NMR}$ (CDCl_3) δ -42.8 (t); HPLC t_R : 6.3, 6.6 min.

3. Results and discussion

We have previously reported the rates of alkaline hydrolysis for the phenyl phosphoramidate derivatives of **1** at room temperature [19–22]. The alkaline hydrolysis profiles of the phosphoramidate analogs of nucleoside monophosphates under acidic, neutral and alkaline conditions were reported by several groups [23–28]. In the present study, we synthesized the corresponding phenyl thiophosphoramidate derivatives in order to evaluate their biological activity as well as their hydrolysis profiles. The synthesis was accomplished by a procedure represented by Scheme 1.

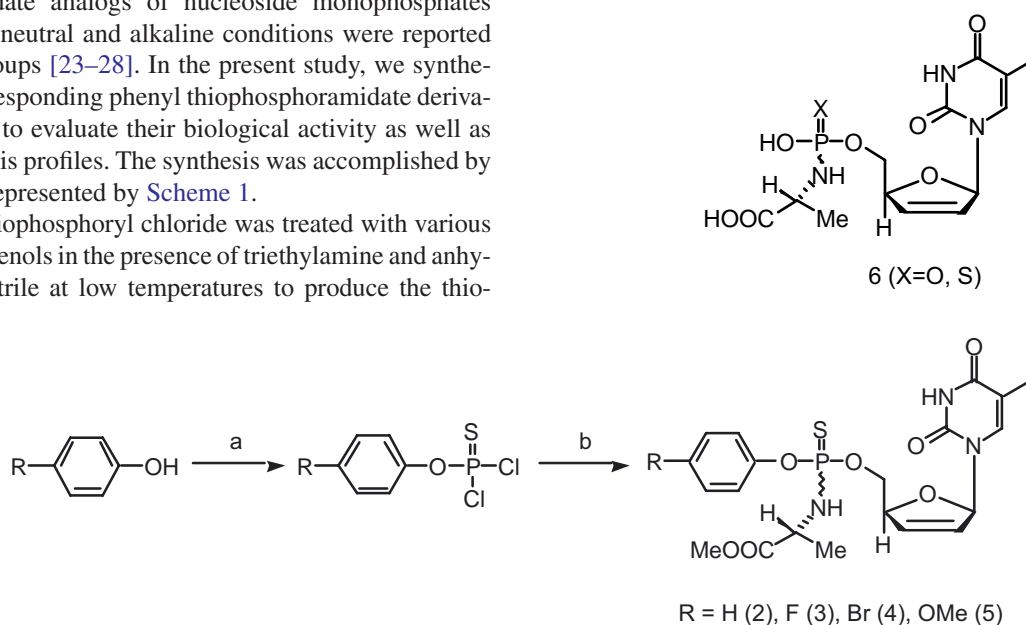
In brief, thiophosphoryl chloride was treated with various substituted phenols in the presence of triethylamine and anhydrous acetonitrile at low temperatures to produce the thio-

phosphorodichloridate. This was treated with L-alanine methyl ester hydrochloride at -78 °C yielding the corresponding thiophosphorochloridate derivatives. In the subsequent step, these derivatives were reacted with **1** in anhydrous acetonitrile in the presence of triethylamine and triazole to obtain the target compounds, which were then purified.

3.1. Alkaline hydrolysis of phosphoramidates and thiophosphoramidates of **1**

In our earlier studies [19–21] we have examined the alkaline hydrolysis of phosphoramidate derivatives of **1** and concluded that the superior biological activity shown by these compounds is due to the rapid formation of an important metabolite, namely the alaninyl monophosphate derivative of d4T (**6**, X = O) [22]. In addition, we have demonstrated that the presence of electron withdrawing groups on the phenyl ring enhances the activity for these phosphoramidate derivatives by improving the rate of hydrolysis. By analogy we have also used an enzyme esterase (in vitro) to further support our assertion that the biological activity of these phosphoramidate derivatives is directly related to their rate of hydrolysis. We [20,22] and others [11,12,27] have reported that the first step involves the hydrolysis of the methylester to the corresponding acid, which simultaneously cyclize and eliminate the phenoxy moiety of the compound that ultimately results in the formation of the most active metabolite, **6** (X = O). However, we could not isolate the intermediate cyclized product to unequivocally decipher the mechanism of elimination of the phenoxy moiety in the structure of these phosphoramidate derivatives.

In the present investigation, we aimed to examine the hydrolysis of thiophosphoramidate derivatives synthesized as shown in Scheme 1. We have determined the rate of



Scheme 1. Synthesis of substituted aryl thiophosphoramidate derivatives of d4T. (a) $\text{PSCl}_3/\text{Et}_3\text{N}$, (b) L-alanine methyl ester, 1,2,4-triazole, Et_3N , **1**.

formation of each of the hydrolysis products to further understanding of the mechanism of alkaline hydrolysis.

Table 1 shows the rate of formation of each of the metabolites at various temperatures during alkaline hydrolysis of stampidine **7**, a bromo-substituted phosphoramidate derivative of **1**. The table also gives the energy of activation (E_a) in kcal mol⁻¹ calculated using the Arrhenius equation. The rate of disappearance of the starting material is found to be slower than the rate of formation of metabolite. This suggests that the first step involving the hydrolysis of methylester to the corresponding acid is a slow step. In the second step the cyclized intermediate product eliminates the phenoxy moiety to form the metabolite and that this step may involve the build up of the intermediate before proceeding. Since multiple steps are involved for the formation of the metabolite and intermediates we are unable to determine the kinetic order of this process. However for simplicity we assumed this process follows first order rate early in the kinetic cycle. The rate of formation for each metabolite increased with temperature as expected. The energy of activation of formation **6** (X = O) was 12.8, 13.1 kcal mol⁻¹ for **1** and 15.1 kcal mol⁻¹ for *p*-bromophenol.

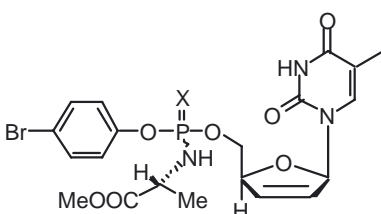
If we compare the rate of formation of **1**, **6**, and *p*-bromophenol as well as the disappearance rate of the starting material from the alkaline hydrolysis of **7** with that of **4**, it is evident that the hydrolysis of the latter was almost 10-fold slower, and the difference in E_a values indicates that thio-

phosphoramidate derivatives are less reactive than the phosphoramidate derivative, and therefore, has a higher transition state energy.

We next examined the hydrolysis profiles of compounds containing an electron donating methoxy group in the phenyl moiety of both phosphoramidate **8** as well as thiophosphoramidate **5** derivatives of **1**. Fig. 1 shows the HPLC chromato-

Table 1

Rate constants and the corresponding energy of activation (E_a) values for the 4-bromo-substituted derivatives

					
X = S (4), O (7)					
Compound	Temperature (°C)	6 ^a	1 ^a	Phenol ^a	Initial compound ^a disappearance rate
7	-10	0.23	0.30	0.05	0.19
	0	0.88	1.14	0.70	0.46
	8	1.58	1.69	0.82	1.25
	15	2.49	2.14	1.33	1.91
	25	4.31	3.07	2.19	4.12
Arrhenius (E_a) ^b	NA	12.8	13.1	15.1	13.9
4	8	0.06	0.04	0.02	0.04
	15	0.27	0.19	0.09	0.07
	25	0.70	0.46	0.16	0.37
Arrhenius (E_a) ^b	NA	24.5	24.9	21.2	23.4

^a Rate constants were calculated using first order rate equations and are expressed in h⁻¹. The values are the average of three independent runs and the error was $\pm 5\%$.

^b Activation energies (E_a) were calculated using the Arrhenius equation and are expressed in kcal mol⁻¹.

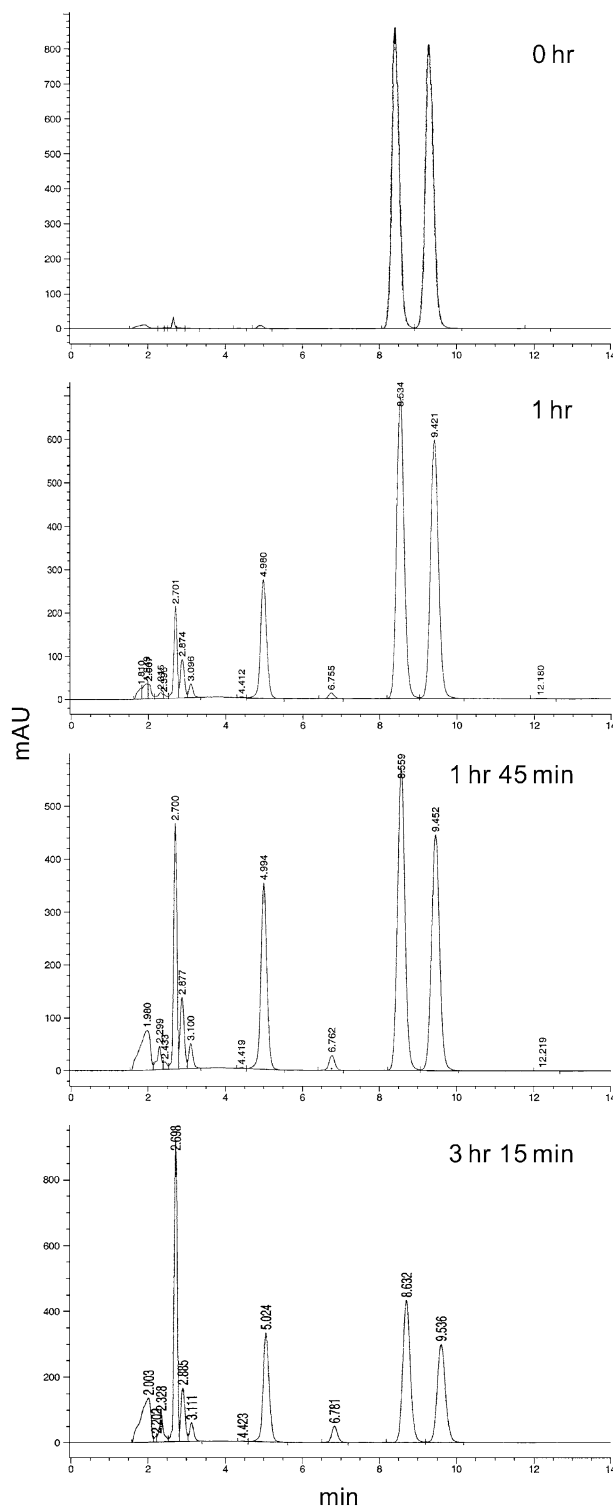


Fig. 1. Kinetics of alkaline hydrolysis for **8** at room temperature.

gram of the reaction between base and phosphoramidate derivative at various intervals of time.

The peak at 8.49 and 9.38 min corresponds to the starting material (distereoisomers) and the peak at 4.98 min represents the methoxyphenol formation. The other peaks in the chromatogram at 2.7 and 1.9 min are those of **6** and **1**, respectively. The retention times of the above are confirmed by comparison with authentic samples of appropriate compounds. At 1 h methoxyphenol, **1** and **6** were detectable. At 3 h, 15 min, almost 50% of **8** was converted into the hydrolysis products. The rate of formation of the hydrolysis products and the E_a values are shown in Table 2.

Overall, the temperature dependent formation of the hydrolysis products was slower for the methoxy-substituted compounds **5** and **8** than for the bromo-substituted compounds **4** and **7** (Tables 1 and 2). This was expected due to the electron donating substituents on the phenyl ring should decrease the hydrolysis rate whereas electron withdrawing groups should increase the hydrolysis rate. As shown in Table 2, the energy of activation for the formation of **6** from the parent **8** was $15.7 \text{ kcal mol}^{-1}$. The energies of activation for all other products were higher than that of **6**.

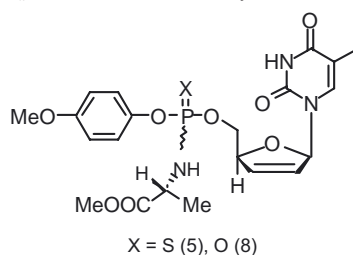
Next we examined the alkaline hydrolysis of **5** at room temperature (Fig. 2). Within 30 min we observed two intermediate peaks in the chromatogram, one at 8.4 min and another at 10.0 min. Formation of these two intermediate products during alkaline hydrolysis of the thiophosphoramidate derivative **5** is in sharp contrast with the results obtained from the phosphoramidate derivative **8** (Fig. 1). In our earlier publications on the hydrolysis profiles of phosphoramidate derivatives of **1** [21], we were unable to observe this intermediate, most likely due to their unstable nature preventing detection under our experimental conditions. Introduction of

a sulfur in place of an oxygen in these phosphoramidate derivatives apparently stabilizes this intermediate. To our knowledge, this is the first time that formation of such an intermediate has been reported during alkaline hydrolysis of thiophosphoramidate derivatives of **1**. Unfortunately, there is no literature precedence for this putative intermediate of thiophosphoramidate analogs of stavudine. The LC/mass spectral data for the two peaks and their proposed intermediate structures are shown in Table 3. Table 2 further shows that the rate of hydrolysis of **5** is faster than **8** at various temperatures. This can be rationalized due to the fact that the thiophosphoramidate derivative reacts by an alternate pathway. Additionally, this result indicates that the rate of intermediate formation is much higher than the formation of other products (Table 2). Several attempts to synthesize these intermediates were unsuccessful due to elimination of the phenoxy moiety. Although one would expect the phenoxy group as the leaving group in preference over the nucleoside moiety during alkaline hydrolysis, the intermediate products retained the phenoxy moiety in their structure (Table 3). The difference in the nucleophilicity between the sulfur and oxygen analogs could account for the differences in the intermediates formed in the reaction. Also, we see the formation of d4T, which demonstrates the tentative structure of the intermediate. Further more the *p*-fluoro substituted thiophosphoramidate derivative gave an intermediate which is different in structure as compared to the other two derivatives. Based on the LC/mass spectral fragmentation the proposed structure seem to be the carboxylic acid. The energy of activation varied from 27 to 36 kcal mol^{-1} for most of the products.

We next synthesized the fluoro-substituted phosphoramidate **9** as well as thiophosphoramidate derivative **3** for comparison. Compound **9** underwent hydrolysis slower com-

Table 2

Rate constants and the corresponding energy of activation (E_a) values for the 4-methoxy-substituted derivatives



Compound	Temperature (°C)	6 ^a	1 ^a	Phenol ^a	Inter. ^a	Initial compound ^a disappearance rate
8	8	0.06	0.05	0.10	NA	0.01
	15	0.20	0.40	0.46	NA	0.06
	25	0.30	0.99	1.59	NA	0.19
Arrhenius (E_a) ^b	NA	15.7	29.4	26.7	NA	27.1
5	8	0.03	0.02	0.05	0.06	0.05
	15	0.19	0.15	0.05	0.33	0.14
	25	0.57	0.39	0.03	0.91	1.34
Arrhenius (E_a) ^b	NA	29.9	26.8	NA	38.6	36.1

Inter. = Intermediate.

^a Rate constants were calculated using first order rate equations and are expressed in h^{-1} . The values are the average of three independent runs and the error was $\pm 5\%$.

^b Activation energies (E_a) were calculated using the Arrhenius equation and are expressed in kcal mol^{-1} .

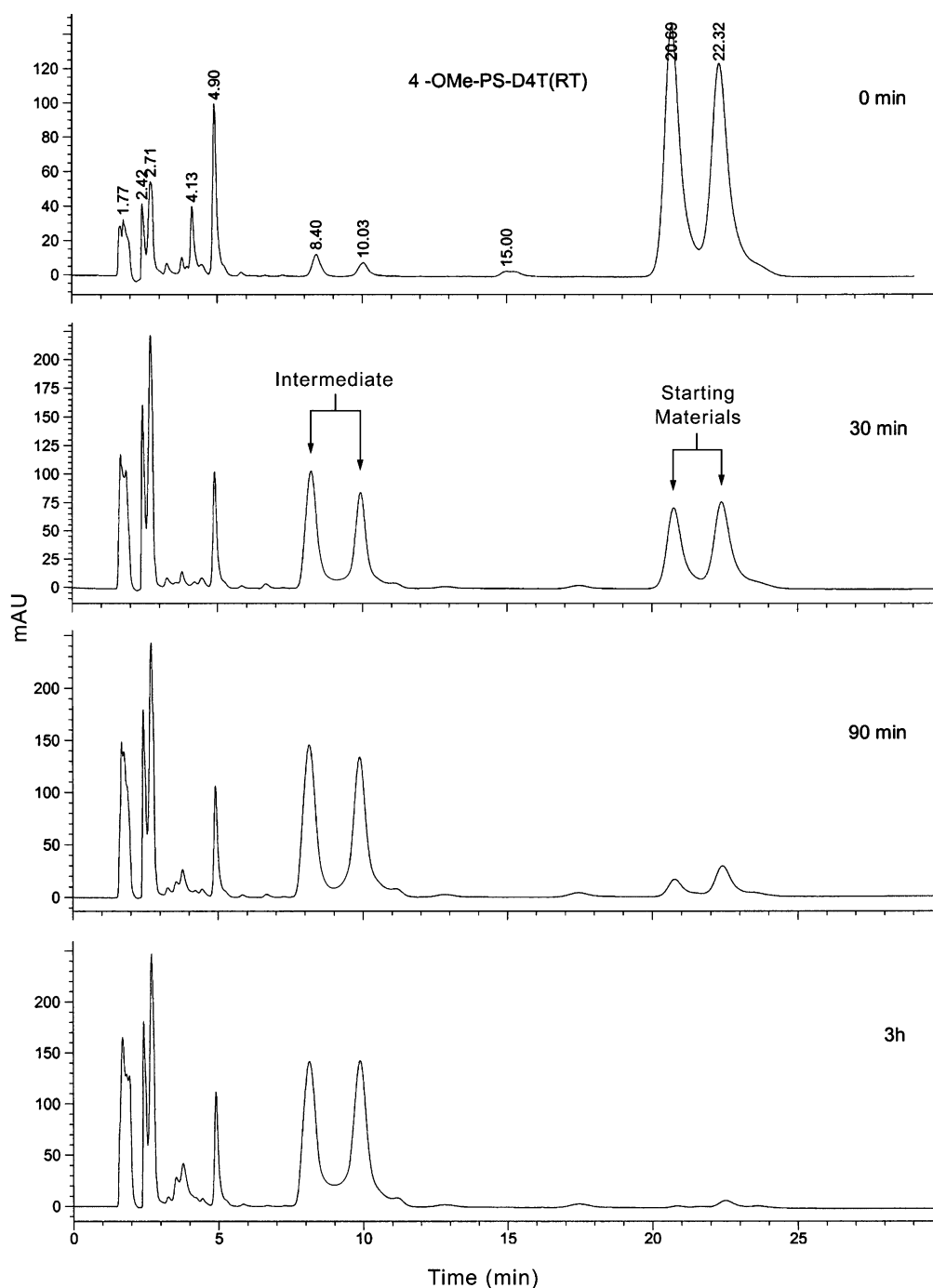


Fig. 2. HPLC profile of compound **5** treated with sodium hydroxide at various time intervals.

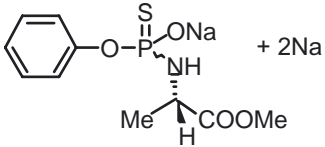
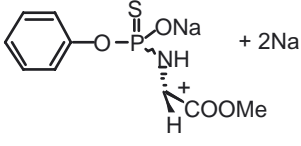
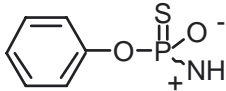
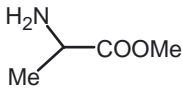
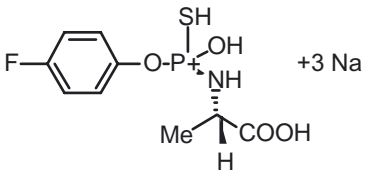
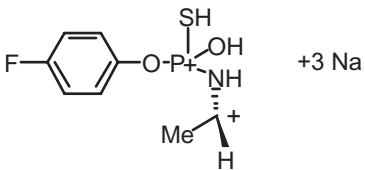
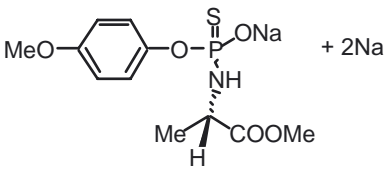
pared to the bromo-substituted compound **7**, which is understandable due to lower electron withdrawing capacity of fluorine as compared to bromine. However, we could not identify any intermediates from the HPLC profiles, a result similar to that observed for the bromo-substituted compound. Table 4 shows the rate of formation of various products for the fluoro-substituted derivative at various temperatures.

The energy of activation varied from 9.5 to 13.7 kcal mol⁻¹ for most of the products. When we examined the

alkaline hydrolysis profiles of fluoro thiophosphoramidate (**3**); we were able to observe the formation of an intermediate product (Fig. 3) similar to that in the case of **5**. Thus, unlike compound **4**, compound **3** yielded the intermediate product.

In order to explain various trends associated with the substitutions on the phenyl ring of these thiophosphoramidates as well as phosphoramidates, we prepared and analyzed the corresponding unsubstituted analogs **2** (Fig. 4) and **10**, respectively (Table 5). We observed the formation of phenol, **1** and **6** (X = O, S) during the alkaline hydrolysis of

Table 3
LC/mass spectral analysis of the intermediate product of thiophosphoramidate derivatives

Compound	Observed mass of intermediate	Tentative structure
2	342 (M – 1)	
	330 (M + 1)	
	187 (M)	
	105 (M + 2)	
3	351 (M + 2)	
	306 (M + 1)	
5	372 (M – 1)	

these unsubstituted compounds. The rates of hydrolysis were slower than those of the compounds with electron withdrawing substituents in the aryl moiety. We found that the energy

of activation was approximately 25 kcal mol⁻¹ for most of the products of the phosphoramidate derivatives (X = O).

There are two possible pathways through which products can result for the phosphoramidate and thiophosphoramidate derivatives (Fig. 5).

Compound **A** forms products **C** and **D** at rate k_1 , or **C** and **D** can be formed through an intermediate **B** with rates k_2 and k_3 . Therefore, the rate of formation of products relates to k_1 and the rate of formation of **B** can be used to derive k_2 . Differences will be observed between **C** and **D** formation if the reaction scheme traverses through **B**. As discussed before caution should be exercised in comparing rate of formation of products and intermediates when the kinetic order is not known. However, our interest was to compare the rate of formation of intermediate and products between phosphoramidate and thiophosphoramidate under similar assumption and experimental conditions.

Using this notation, we conclude that in the case of phosphoramidate compounds (X = O), lack of detection of intermediate forces us to assume that the reaction proceeds by forming **C** and **D** directly. On the other hand in the case of thiophosphoramidate derivatives we were able to observe the formation of intermediate **B**. These steps are further illustrated through the transition state diagram shown in Fig. 6.

Thus, the presence of sulfur instead of oxygen in the structure of phosphoramidate derivatives greatly influences the pathway through which the products are formed during hydrolysis.

To further understand the thermodynamic factors associated with hydrolysis pathway between phosphoramidate and thiophosphoramidate derivatives, we evaluated Gibbs free energy as well as enthalpy for phosphoramidates and thiophosphoramidates. We initially obtained the energy of activation by using Arrhenius equation:

$$\log k = \log A - E_a/2.303RT \quad (1)$$

where, k represents the specific reaction rate, A is a constant, E_a is the energy of activation, R is the gas constant (1.987 cal deg⁻¹ mol⁻¹) and T is the absolute temperature. Plotting $\log k$ vs. $1/T$ we were able to obtain the slope of the line that in turn gives the following Eq. (2) comprising energy of activation:

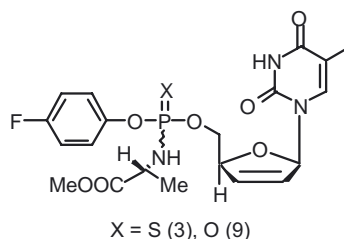
$$\text{Slope} = -E_a/2.303R \quad (2)$$

We next invoked the transition state theory, or absolute rate theory, according to which an equilibrium is considered to exist between the normal reactant molecule and an activated complex of these molecules. Subsequent decomposition of the activated complex leads to product. For an elementary bimolecular process, the reaction may be written as:



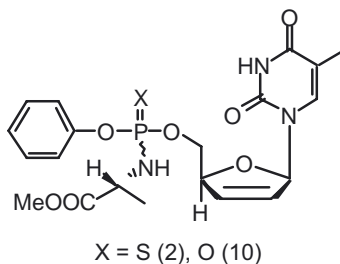
The double dagger is used to designate the activated state. In principle, the transition state theory gives the influence of

Rate constants and the corresponding energy of activation (E_a) values of the 4-fluoro substituted derivatives



Compound	Temperature (°C)	6 ^a	1 ^a	Phenol ^a	Inter. ^a	Initial compound ^a disappearance rate
9	8	0.45	1.18	0.35	NA	0.73
	15	1.01	2.17	0.95	NA	1.32
	25	1.52	3.16	1.31	NA	2.94
Arrhenius (E_a) ^b	NA	11.7	9.6	12.7	NA	13.7
3	8	0.04	0.02	0.01	0.07	0.02
	15	0.09	0.06	0.03	0.14	0.07
	25	0.34	0.18	0.09	0.42	0.18
Arrhenius (E_a) ^b	NA	21.7	19.6	20.2	17.4	21.8

^a Rate constants were calculated using first order rate equations and are expressed in h^{-1} . The values are the average of three independent runs and the error was $\pm 5\%$.

Rate constants and the corresponding energy of activation (E_a) values of the unsubstituted derivatives

Compound	Temperature (°C)	6 ^a	1 ^a	Phenol ^a	Inter. ^a	Initial compound ^a disappearance rate
10	8	0.08	0.08	0.09	NA	0.02
	15	0.53	0.34	0.51	NA	0.08
	25	1.14	1.08	1.25	NA	0.21
Arrhenius (E_a) ^b	NA	24.3	25.7	25.2	NA	23.5
2	8	0.05	0.10	0.01	0.16	0.01
	15	0.08	0.25	0.03	0.29	0.07
	25	0.27	0.52	0.05	0.99	0.15
Arrhenius (E_a) ^b	NA	16.7	15.7	18.1	18.1	23.3

^a Rate constants were calculated using first order rate equations and are expressed in h^{-1} . The values are the average of three independent runs and the error was $\pm 5\%$.

where R is the gas constant, T being the absolute temperature, N is Avogadro's number and h is Plank's constant. Using the

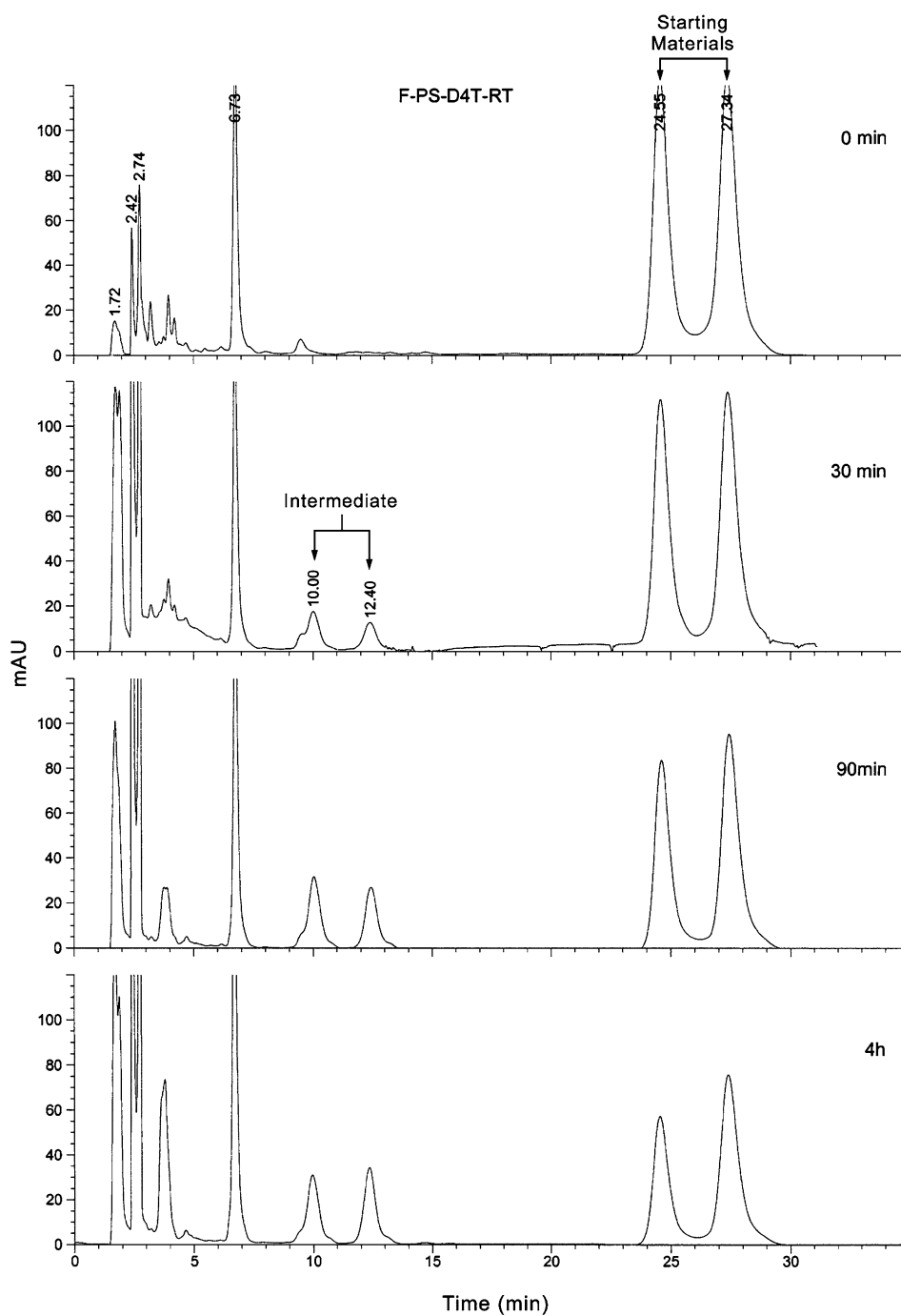


Fig. 3. HPLC profile of compound 3 treated with sodium hydroxide at various time intervals.

above equations and following the chemical principles such as:

$$\Delta G = \Delta H - T\Delta S \quad (5)$$

we were able to calculate the E_a , ΔG and $T\Delta S$ for these derivatives.

3.2. Relationship between σ and E_a for phosphoramidate and thiophosphoramidate derivatives

We explored the relationship between Hammett sigma (σ) [29] and the energy of activation obtained for each set of the previously discussed compounds to find out whether any correlation exists among the substituents and $E_a/T\Delta S$. The

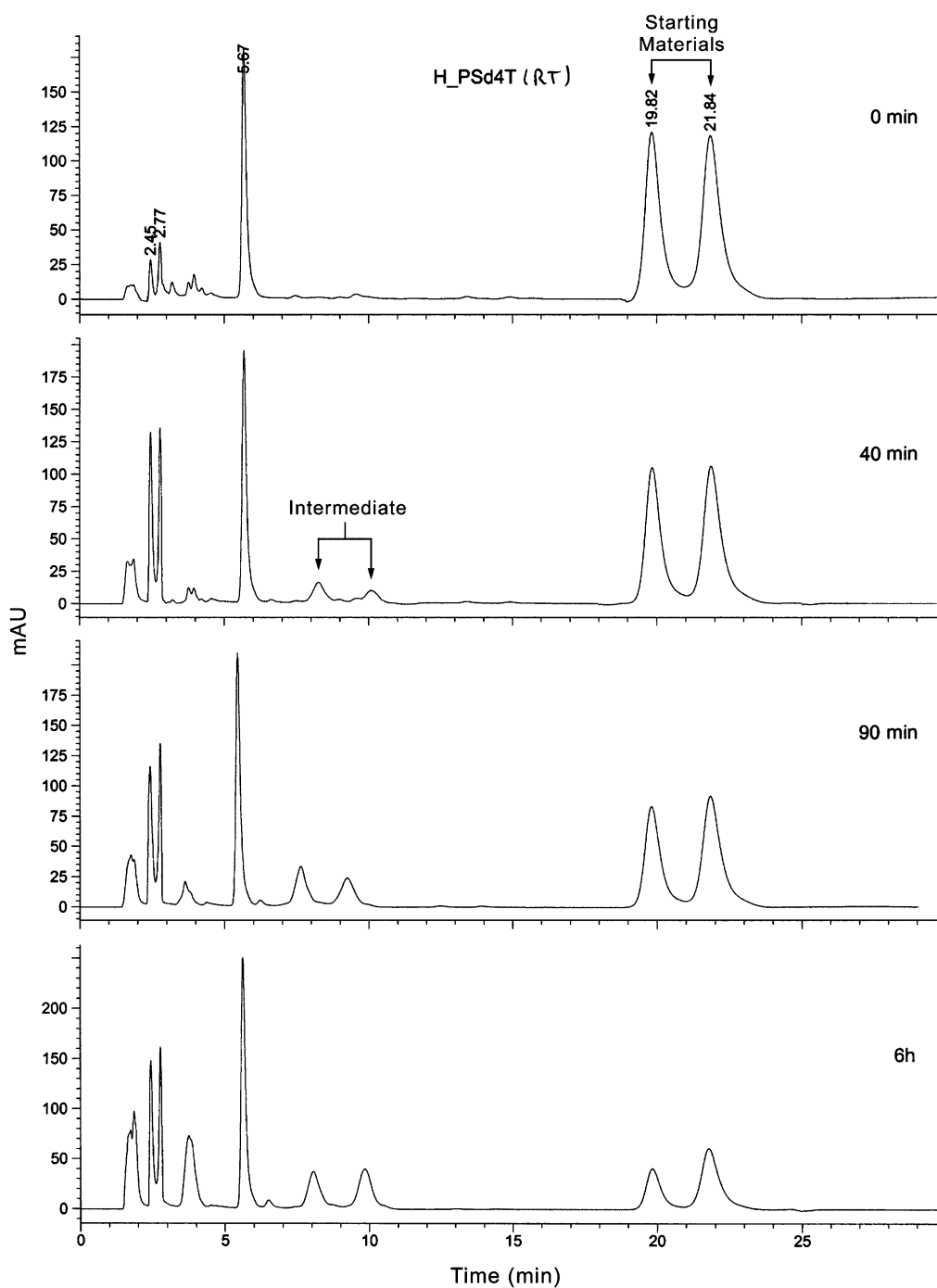


Fig. 4. HPLC profile of compound 2 treated with sodium hydroxide at various time intervals.

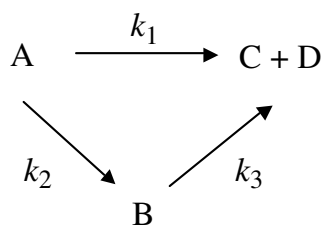


Fig. 5. Pathways for alkaline hydrolysis of phosphoramidates and thiophosphoramidates.

analysis of covariance (ANCOVA) model [30] significantly predicted $T\Delta S$ values ($R^2 = 0.85$, $F(2,5) = 13.68$, $P = 0.0094$). There was a significant effect of the covariate sigma ($P = 0.0064$) and $X = S/X = O$ categorical group ($P = 0.045$). The variance explained by the sigma covariate (F -ratio = 20.2) was greater than the effect of $X = S/X = O$ group (F -ratio = 7.1). Therefore, the difference between $X = O$ and $X = S$ is significant when the sigma values are taken in to account. A similar effect profile was observed with E_a values (Fig. 7; $R^2 = 0.87$, $F(2,5) = 16.53$, $P = 0.0063$). There was a significant effect of the sigma covariate ($P = 0.0045$) and the

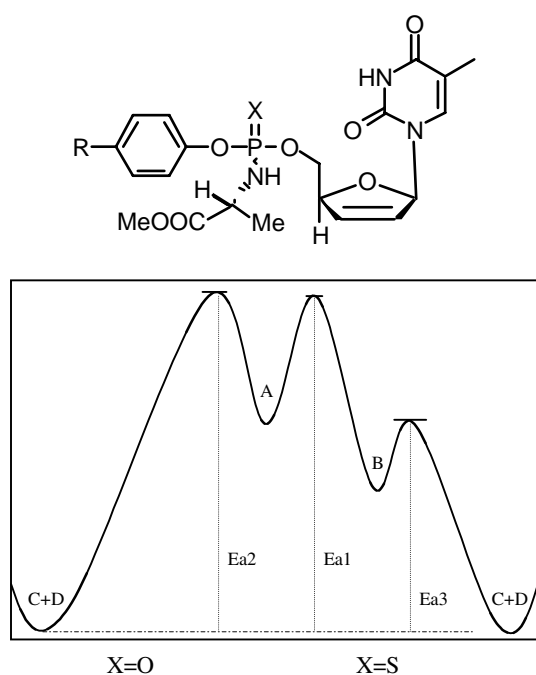


Fig. 6. Transition state diagram for aryl substituted phosphoramidate and thiophosphoramidate derivatives of **1**.

X = S/X = O group category ($P = 0.029$) in predicting E_a values. Fig. 7 shows the negative correlation between E_a and sigma for both X = O (Fig. 7a) and X = S compounds (Fig. 7b; $R^2 = 0.78$). High proportion of the variance was also explained for X = O (0.88) and X = S (0.76) with respect to $T\Delta S$.

The amount of variance explained by Hammett sigma was expressed as R^2 values. Fig. 7 shows that more variance was explained by Hammett sigma for phosphoramidates than thiophosphoramidates. The reduced correlation between σ and E_a for the thiophosphoramidates may be due to competing pathways for these compounds.

Table 6 shows the energy of activation (E_a) and entropy values ($T\Delta S$) obtained for various substituted phosphoramidate and thiophosphoramidate derivatives of **1** (the Gibbs free energy values varied between 21 and 23 kcal mol⁻¹ for most of the derivatives, not shown).

From the table values it is evident that the free energy of activation values varied from 14 to 36 kcal mol⁻¹ depending on the substituents on the phenyl ring. Also the thiophospho-

ramidate showed a higher energy of activation compared to phosphoramidate derivatives. The most striking difference is the entropy of the reaction, which is represented in the table as $T\Delta S$. For electron withdrawing substituents such as bromo and fluoro groups a negative value with a magnitude of -7 kcal mol⁻¹ for the phosphoramidate derivatives was observed, while the electron donating group gave a value of +3.8 kcal mol⁻¹. The variation of $T\Delta S$ values for the thiophosphoramidate derivatives were significantly less with the exception of the methoxy substituent, which showed a value of +13.9 kcal mol⁻¹.

3.3. ³¹P-NMR studies on the reaction between phosphoramidate and sodium hydroxide

We next set out to find by NMR what products are observed during the reaction. The sample was dissolved in a minimal amount of deuterated methanol and to this was added sodium hydroxide solution and the NMR spectrum was taken after various time intervals. A capillary containing 1% phosphoric acid in water served as an internal standard, which was adjusted to 0 ppm. Table 7 depicts selected chemical shift values observed for various compounds.

We chose the phosphoramidates with electron withdrawing substituents as these compounds could be hydrolyzed faster. The phosphoramidate derivatives were obtained as distereoisomers consisting of both "R" and "S" isomers due to the chirality at phosphorus center. In general a 40:60 enantiomeric ratio was obtained for all the derivatives. The two peaks corresponding to each isomer of the diastereomeric mixture of the **7** was observed at 4.56 and 4.4 ppm, respectively, relative to the standard phosphoric acid positioned at 0 ppm. Within 3 h we were able to observe the completion of the reaction and the ³¹P-NMR showed five major peaks in the spectrum. In the second experiment, we used a single isomer of the bromo-substituted phosphoramidate derivative, which showed a peak at 4.4 ppm at 0 min. In 1 h we once again observed five peaks corresponding to five different compounds. The chemical shift values observed (after giving allowance for the minor change in shift values due to sample character) were similar to those obtained for the distereoisomeric mixture. This demonstrates that the final product of hydrolysis in both cases loses chirality during the reaction, otherwise we would have observed marked differences in the chemical shift values for the above two experiments.

To further confirm our results from the NMR studies, we used cyano-substituted as well as 2,5-dichloro-substituted phosphoramidate derivatives (**11** and **12**, respectively) and found that the final products had similar chemical shifts as that of **7**, once again indicating that they all form the same hydrolysis products.

The peaks at 10.4 and 10.5 ppm observed in each of the cases (see Table 7 for further details) may be attributable to an intermediate that eventually is hydrolyzed in the medium to give the final stable products. Considering the HPLC

Table 6

Experimentally determined values for energy of activation (E_a), and entropy ($T\Delta S$) for the disappearance of starting material at 25 °C

Compound	E_a (kcal mol ⁻¹)	$T\Delta S$ (kcal mol ⁻¹)
7	13.9	-7.5
4	23.4	+0.5
9	13.7	-7.9
3	21.7	-1.6
10	23.5	+0.3
2	23.2	-0.2
8	27.1	+3.8
5	36.1	+13.9

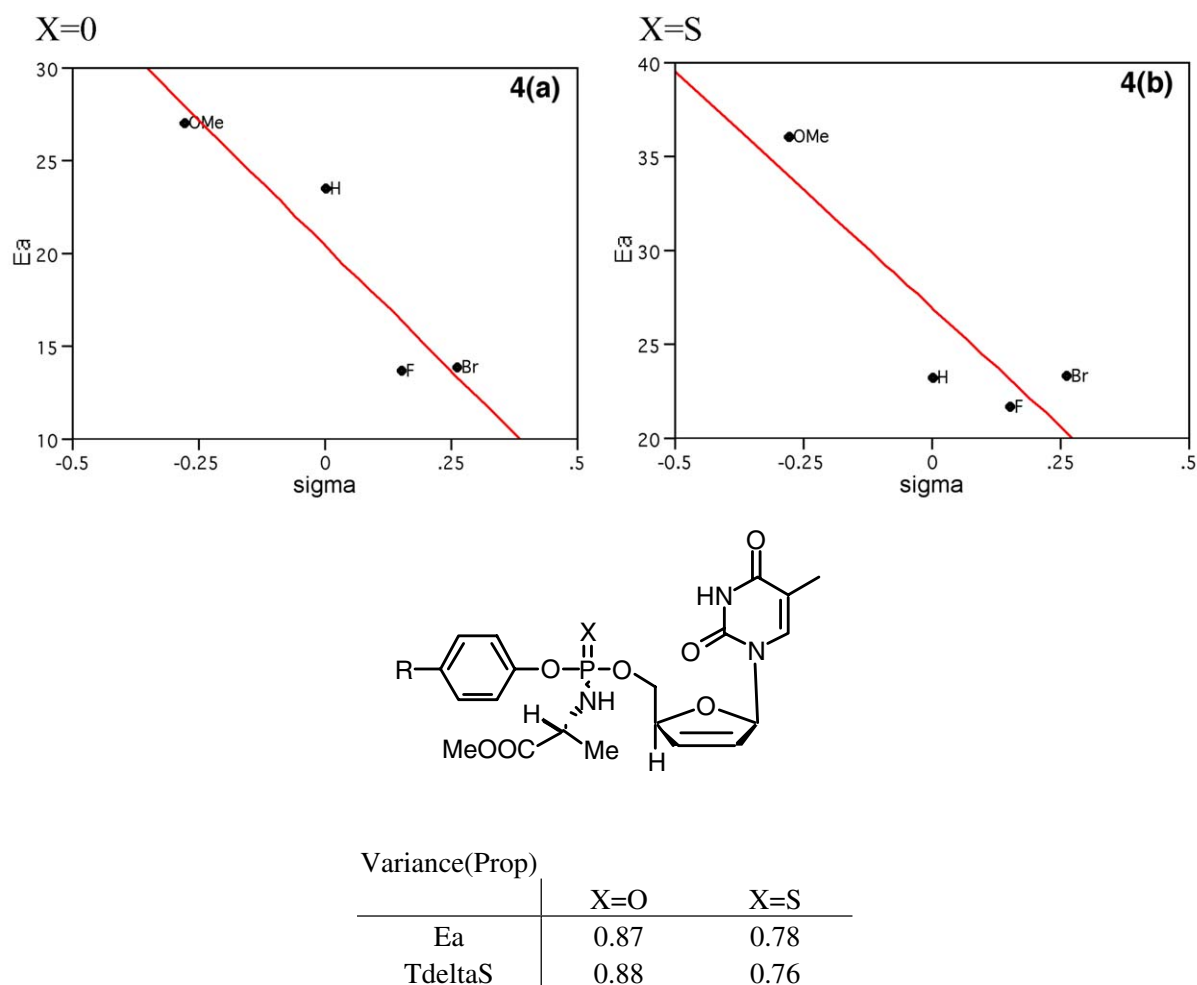
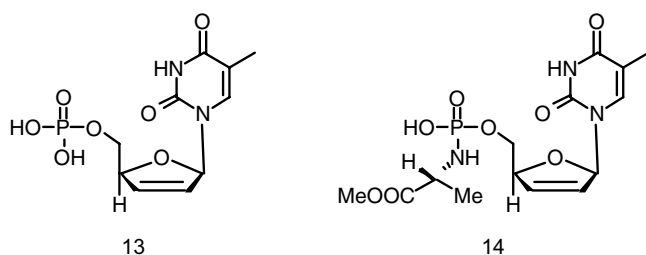


Fig. 7. The effect of sigma for sulfur and oxygen substituted compounds on the energy of activation (E_a). The ANCOVA model significantly predicted E_a values ($P = 0.0063$). There was a significant effect of sigma ($P = 0.0045$) and $P = S/P = O$ group substitution ($P = 0.029$). The effect of sigma (F -ratio = 23.9) was greater than the effect of $X = S/X = O$ group (F -ratio = 9.2). Relationship between E_a and sigma values are shown for $X = O$ (a) and $X = S$ (b) substituted compounds. Data points are labeled according to the 'R' substitution.

(Fig. 8) and the NMR spectroscopy results, the products can be proposed as d4T phosphate **13** at 1.71 ppm, d4T methoxy alaninyl monophosphate **14** at 6.23 ppm, and **6** at 7.2 ppm.



Formation of **14** could occur by a nucleophilic substitution reaction with the base. Formation of **6** could occur by hydrolysis of the methyl ester group to the carboxylic acid and subsequent cyclization and simultaneous elimination of the phenoxy moiety. Further hydrolysis of the cyclic intermediate furnishes **6**. Comparing the results obtained from HPLC, Fig. 8 shows the HPLC profile of compound **7** treated with sodium hydroxide at various time intervals. The peak at 7–8 min corresponds to the starting material and peak at

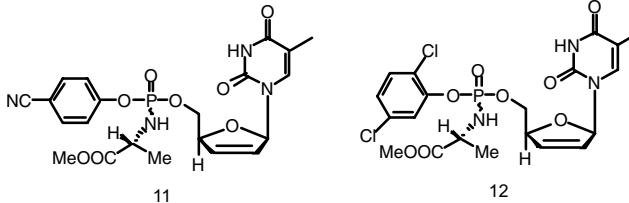
3.8 min represents d4T alanine mono phosphate methylester. Peaks at 2.6, 2.4 and 1.7 corresponds to d4T alanine monophosphate, d4T monophosphate and d4T, respectively. As the time progressed, the starting material depletes resulting in the formation of products. In addition, formation of *p*-bromophenol is evident (13.4 min) after 5 min of reaction. The above results are consistent with those observed in NMR experiments.

3.4. ^{31}P -NMR studies on the reaction between thiophosphoramidate and sodium hydroxide

We next sought to determine the structure of the intermediates obtained in thiophosphoramidate derivatives using ^{31}P -NMR technique. For this purpose we chose compound **5** and treated with sodium hydroxide. The starting material gave two distinct peaks at –11.8 and –12.3 ppm relative to phosphoric acid as internal standard at 0 ppm. After 3 h of treatment with sodium hydroxide the NMR spectrum showed only starting material. Leaving the reaction for additional 14 h at room temperature yielded an additional peak at 3.53 ppm although the major peak was that of the starting

Table 7

³¹P-NMR chemical shifts obtained for P = O compounds during alkaline hydrolysis

		
Compound	Time	Chemical shifts (ppm)
7 (Both isomers)	0	4.6, 4.4
	3 h	6.0, 7.0, 10.6, 11.0, 11.3
7 (Single isomer)	0	4.4
	1 h	6.1, 7.3, 10.6, 11.0, 11.3
11 (Both isomers)	0	4.3, 4.2
	10 min	4.0, 4.1, 6.1, 7.3, 10.4, 10.5
	4 h	4.1, 6.1, 7.3, 10.4, 10.5, 11.0 ^a , 11.3 ^a
	48 h	5.9, 7.0, 10.2 ^a , 10.4 ^a , 10.9, 11.1
12 (Both isomers)	0	4.5
	10 min	4.5, 6.1, 10.4, 10.6
	1.5 h	6.1, 10.4, 10.6, 11.0, 11.3
	36 h	6.1, 7.3, 11.0, 11.3

^a Trace amounts observed relative to the other peaks.

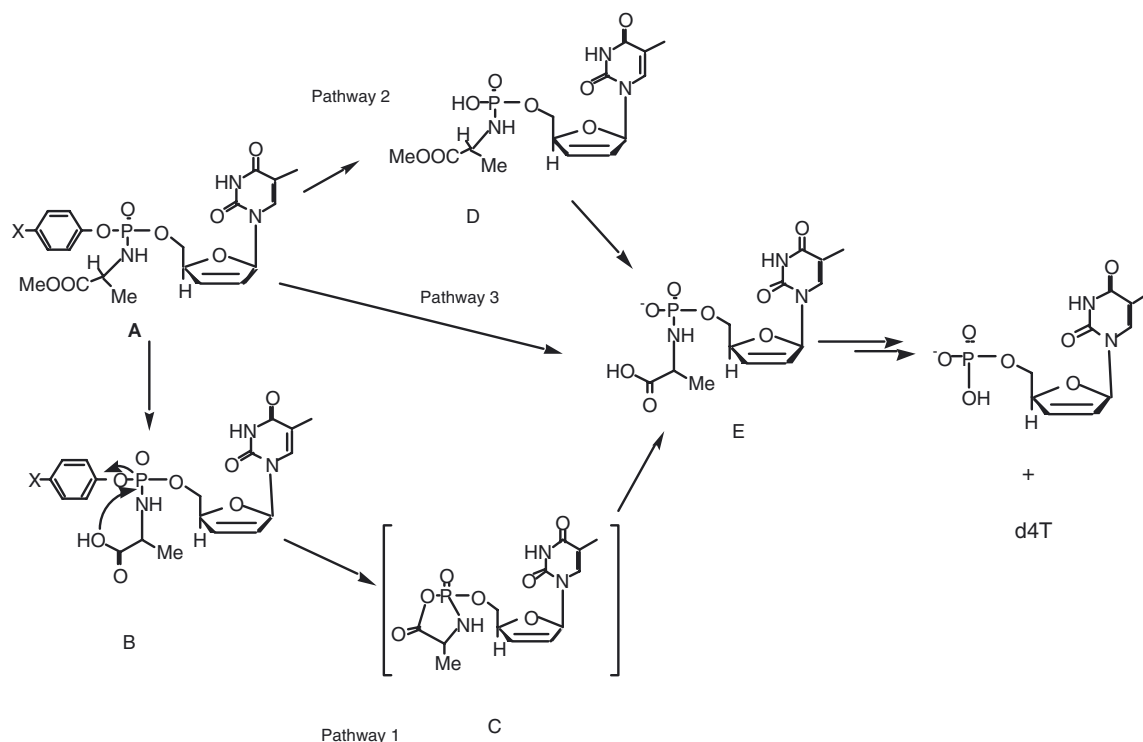
material. The reaction was very slow and hence we were not able to observe any additional peaks with prolonged time of treatment unlike HPLC. Due to the slow reaction times we did not proceed further to identify products of reaction. Our main goal was to find out the differences between thiophosphoramidate and phosphoramidate derivatives under identical conditions and relate them to biological activity.

Based on the products of hydrolysis, we propose the following [Scheme 3](#) for base catalyzed reaction of phosphoramidate derivatives of stavudine.

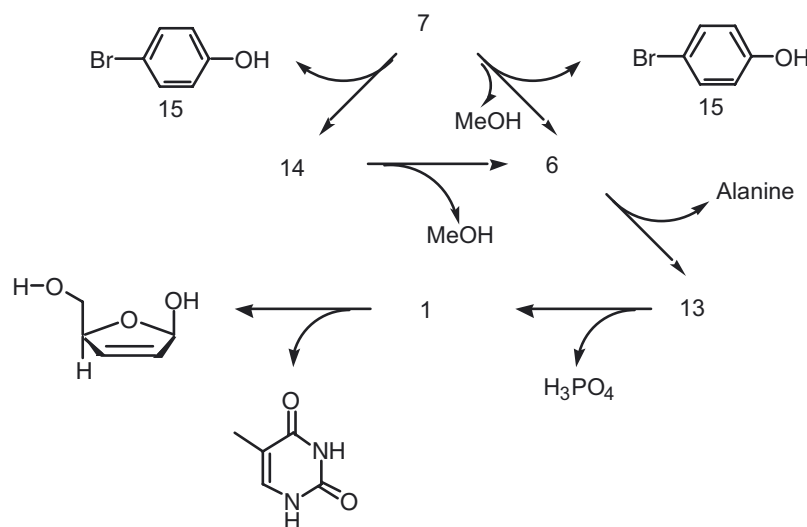
[Scheme 2](#) illustrates various pathways through which products can be formed during alkaline hydrolysis of phosphoramidate derivatives of stavudine. If we consider step-wise mechanism, the ester side chain is first hydrolyzed to carboxylic acid to form intermediate **B**. This intermediate forms cyclic phosphoramidate by elimination of phenoxy moiety intramolecularly resulting in compound **C** which on subsequent hydrolysis by water converts to product **E**. Alternatively, Compound **D** can be formed by direct attack of nucleophile on the phosphorus center, which subsequently gets hydrolyzed by excess base to form compound **E**. A third possibility is that simultaneous attack on the ester side chain as well as on the phosphorus center to produce compound **E**. Ultimately **E** gets converted into d4T monophosphate and d4T.

3.5. Enzymatic hydrolysis studies using porcine liver esterase

In Section 1, we have stated that of the various pro-drug approaches, amino acid phosphoramidate derivatives have shown promise as potent antiviral agents, since in some cases they exhibited enhanced antiviral activity and reduced cytotoxicity when compared to the parent nucleosides [11,12,23]. In order to explain the parameters governing the extracellular and intracellular activation of phosphoramidates, a decomposition pathway of these nucleosides has been proposed and is represented by [Scheme 3](#).



Scheme 2. Possible hydrolysis pathways for phosphoramidate derivative of stavudine in presence of alkali.



Scheme 3. Enzymatic reaction products of aryl phosphoramidate derivatives of **1**.

This scheme represents the pathways through, which various products can be rationalized for these phosphoramidate derivatives. In the first step, carboxyesterase was found to react with **7** to furnish the carboxylic acid by the elimination of methanol, which then cyclizes and intramolecularly eliminates *p*-bromophenol **15** forming an unstable cyclic mixed anhydride. The cyclic anhydride hydrolyses back to the carboxylic acid producing **6**. Alternatively, hydrolysis of the *p*-bromophenol could occur through direct nucleophilic attack by hydroxide ion to furnish **14**. This could undergo further hydrolysis to furnish **6**. In in vivo experiments we have discovered that *p*-bromophenol converts into *p*-bromophenylsulfate by the action of a sulfatransferase [22]. Further steps involving phosphodiesterase produces the nucleoside monophosphate **13**, which in the presence of a phosphatase finally converts into **1**.

We also examined the esterase-mediated hydrolysis of **7** to prove the formation of the carboxylic acid product **6**. For this purpose we utilized HPLC technique. Fig. 9 shows the HPLC profiles of reaction products of **7** after treatment with porcine liver esterase.

By varying the concentration of the substrate and keeping the enzyme concentration constant we were able to get evidence that indeed the esterase hydrolyses the methyl ester. This is observed by the decrease in the concentration of the starting material. The products were identified using authentic samples synthesized independently for this purpose. In addition, for the first time, we observed that one of the isomers was hydrolyzed faster than the other as evidenced from the values measured for the area under the curve for individual peaks. The implication of such a differentiation caused by the enantioselective reactivity of this enzyme towards the distereoisomers will be the subject of future investigations. Further proof of formation of **6** came from the NMR spectroscopy studies.

NMR identification of the product during reaction between esterase and **7** was achieved using ³¹P-NMR chemical shifts. The experimental details for this study are given in

Section 5. Fig. 10 shows the ³¹P-NMR spectra for compound **7** in presence of esterase at different time intervals.

The chemical shift of the starting material (a diastereomeric mixture) was found to be 4.58 and 4.09 ppm, respectively (Fig. 10A). Addition of esterase to the solution resulted in formation of a distinct peak at 6.76 ppm relative to the standard within 2 h (Fig. 10C). After 6 h there was no change in the NMR spectrum, (Fig. 10D) indicating that only one product was formed in the reaction mixture. The product was identified independently by running the authentic sample under similar conditions. It is interesting to note that formation of one product demonstrates that the phenolic moiety in the compound is eliminated to furnish **6**. This is in accordance with the results obtained from HPLC experiments, which further substantiates the proposed mechanism of action of enzyme esterase towards these phosphoramidate derivatives of **1**.

3.6. Antiviral activity of aryl phosphoramidate and aryl thiophosphoramidates of **1**

In our earlier discussion, we demonstrated that thiophosphoramidate derivatives had a higher energy of activation for hydrolysis. As such we were interested, if this was related to the biological activity using the antiviral activity profiles for both the derivatives. Fig. 11 shows a histogram of the IC₅₀ values for four sets of compounds from each series.

All the aryl substituted phosphoramidates had IC₅₀ values in the 1–3 nM range, whereas the corresponding thiophosphoramidate analogs had IC₅₀ values in the 1–8 μM range. Notably, **7** and **9** were more potent than **8** and **10** implying that electron withdrawing substituents have beneficial effect. Based on the results obtained from their rate of hydrolysis and energy of activation, we propose that the decrease in potency of the sulfur analogs can be attributed to their higher energy of activation for hydrolysis during the formation of the active metabolites.

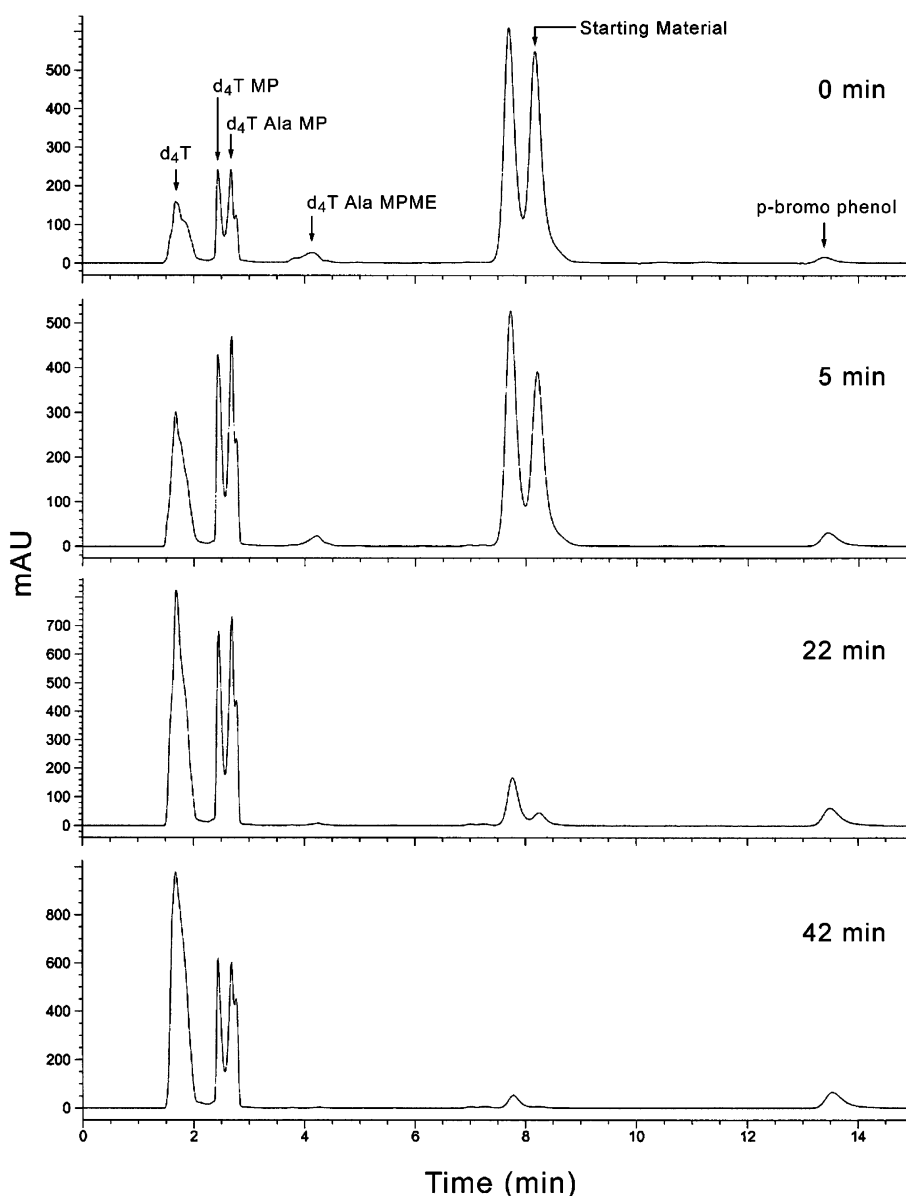


Fig. 8. HPLC profile of compound **7** treated with sodium hydroxide at various time intervals.

4. Conclusions

A comparative study between aryl phosphoramidate as well as aryl thiophosphoramidate derivatives of 2',3'-didehydro-2',3'-dideoxythymidine (d4T, **1**) demonstrated that the replacement of oxygen with sulfur in their structural framework decreases the rate of alkaline hydrolysis by two-fold. In addition, the activation energy (E_a) for the thiophosphoramidate analog was comparatively higher than that of the phosphoramidate analogs. We have also found for the first time that an intermediate is formed in the hydrolysis of the thiophosphoramidate derivatives. Using both HPLC and ^{31}P -NMR techniques, the products of the hydrolysis reaction were identified. We have also correlated Hammett sigma values to the energy of activation and came to the conclusion

that phosphoramidate derivatives show a better correlation as compared to thiophosphoramidates. In addition, we have also demonstrated using our experimental results that enthalpy values vary between phosphoramidate and thiophosphoramidate derivatives. Comparison of anti-HIV activity of aryl phosphoramidate with aryl thiophosphoramidate derivatives of **1** demonstrated that the former derivatives showed 1000-fold more potent antiviral activity. Although it is possible that the reason why the thiophosphoramidates are less potent than the phosphoramidates in the cellular studies is because their conversion to the triphosphate is slow. Alternatively, thiophosphoramidates may function as poor substrates for the kinase enzymes. However, our results suggest that the energy of activation of hydrolysis of these phosphoramidate derivatives play a significant role in their biological potency.

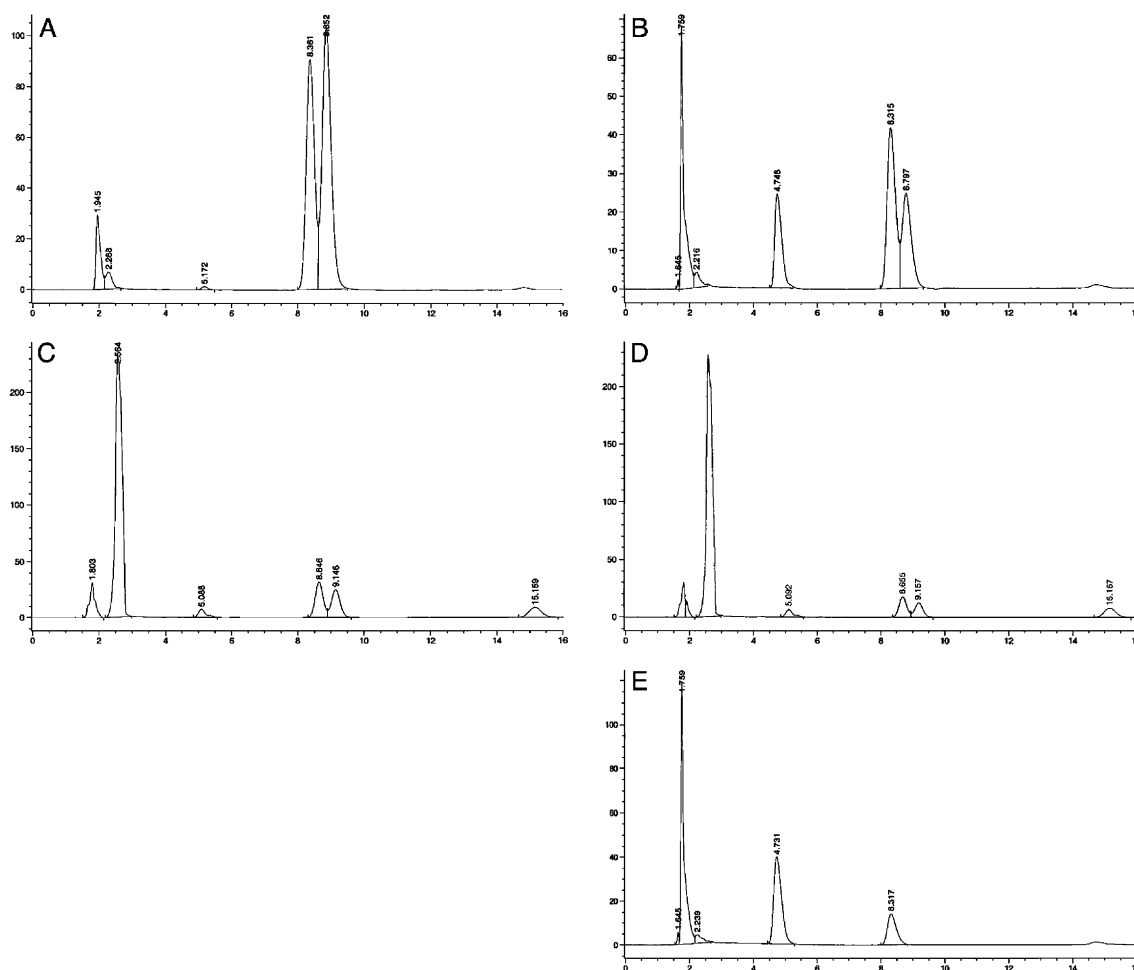


Fig. 9. HPLC profiles of reaction between varying concentrations of **7** and esterase. A. No enzyme; B. 50 µl enzyme + 75 µl of **7**; C. 50 µl enzyme + 60 µl of **7**; D. 50 µl enzyme + 50 µl **7**; E. 50 µl of enzyme + 40 µl of **7**.

5. Experimental protocols

5.1. A general procedure for the kinetic study for alkali hydrolysis of phosphoramidate and thiophosphoramidate derivatives of d4T as monitored by HPLC

A known amount of the phosphoramidate or thiophosphoramidate derivative was carefully weighed (3–4 mg) using an analytical balance and transferred into a scintillation glass vial, 3 ml of methanol were added and the contents were vortexed for 2 min until a homogenous solution was obtained. A 0.05 N NaOH solution was prepared in a volumetric flask using analytical grade NaOH pellets and deionized water. A 1 ml aliquot from the stock solution of the compound was pipetted out into another glass vial. To this vial 0.350 µl of 0.05 N NaOH was added from the volumetric flask using a pipette. The contents were mixed thoroughly by shaking the vial. From this mixture 50 µl was used for HPLC analysis. The column used was a Lichrospher RP-18 analytical column of 4 × 250 mm. The eluent used for HPLC was water (0.1% TEA + 0.1% TFA)/acetonitrile (65:35). The column was maintained at room temperature. The flow rate was maintained at 1 ml min⁻¹, the detection wavelength was

adjusted to 265 nm and the reference wavelength was kept at 400 nm. Aliquots of the sample were drawn from the reaction vial at various time intervals and analyzed. For the fast reactions two HPLC instruments were used simultaneously to determine the rates. Reactions at various temperatures were conducted by keeping the reaction vessel in a constant temperature bath. In the case of low temperature studies, the reaction vial was left in the refrigerator and the temperature of the refrigerator was monitored using a thermometer. Reactions conducted at 0 °C were carried out using external ice bath and those with –10 °C were performed by keeping the reaction vial in a constant temperature freezer.

5.2. A general procedure for the estimation of products from the kinetic study for alkali hydrolysis of phosphoramidate and thiophosphoramidate derivatives of d4T

The amount of products observed during the reaction of the phosphoramidates and thiophosphoramidates were estimated from the area obtained from the HPLC profiles. In addition, when possible authentic samples of the products were run to identify the peaks observed during the reaction.

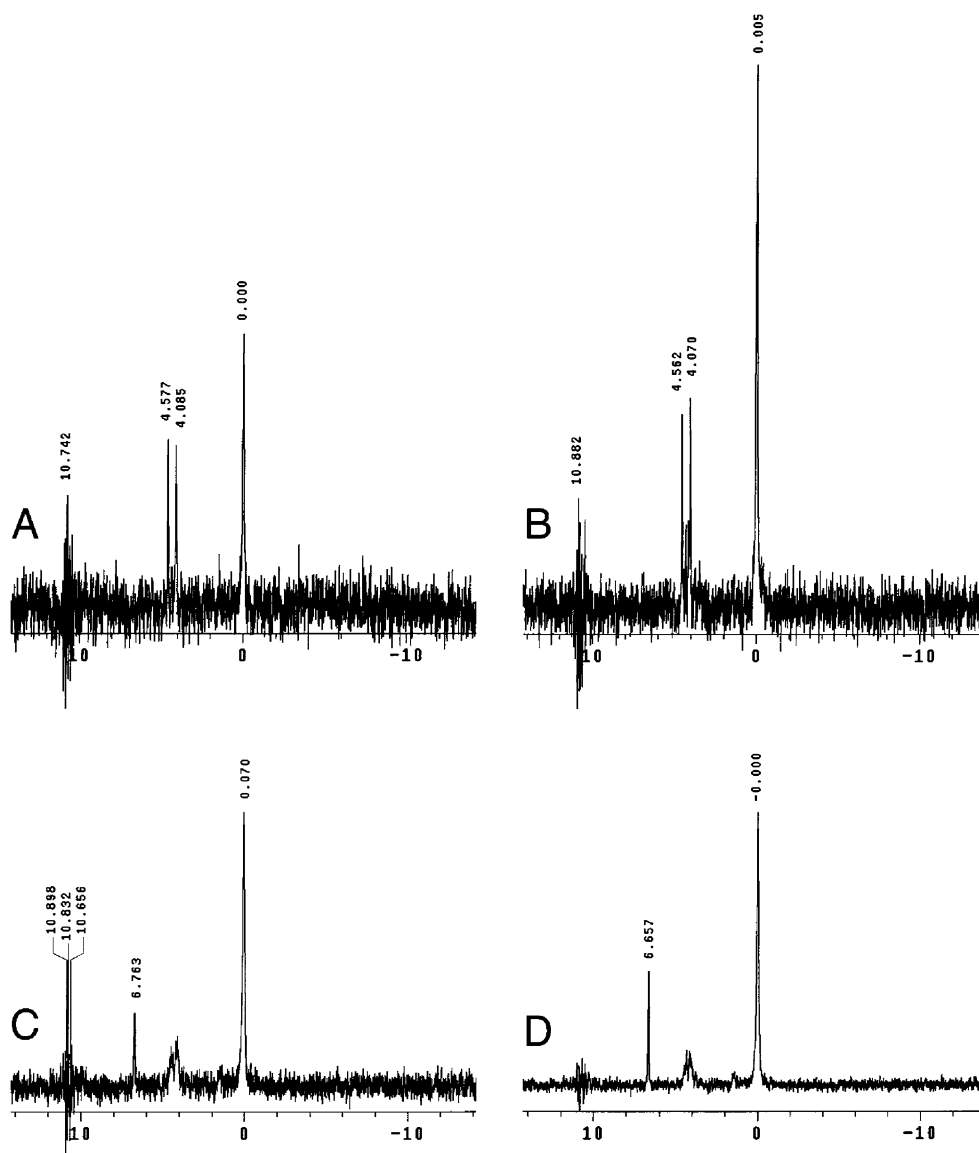


Fig. 10. ^{31}P -NMR profiles of **7** with esterase enzyme at varying intervals of time (peak at 0 ppm represents the phosphoric acid standard in a fused capillary). A: No enzyme; B: after 2 min of addition of enzyme; C: after 2 h; D: after 6 h.

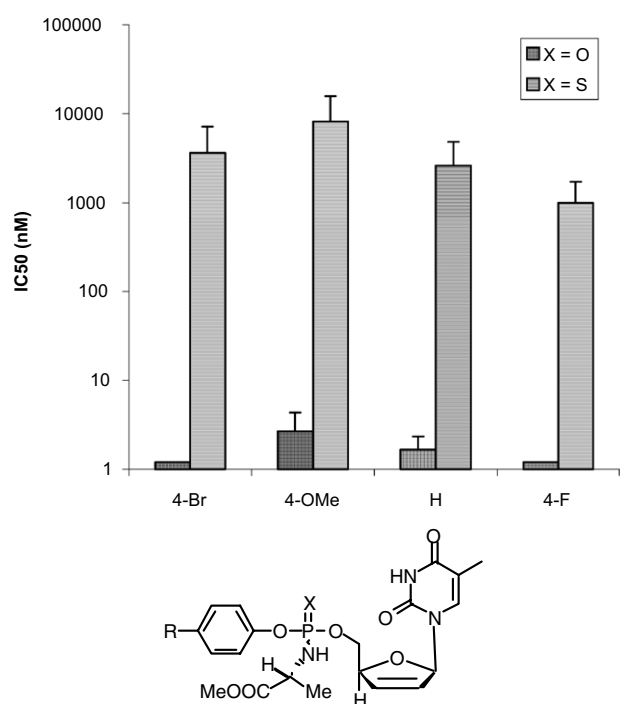
Further confirmation of the product structures were obtained using LC/mass instrument.

5.3. General method for the enzymatic reactions of phosphoramidate and thiophosphoramidate derivatives of d4T as monitored by ^{31}P -NMR spectroscopy

^{31}P -NMR studies with enzyme were conducted using a 5 mm NMR tube. The sample was dissolved in deuterated methanol (100 μl), followed by D_2O (0.4 ml) and then transferred into the NMR tube using a Pasteur pipette. The capillary tube containing a 1% phosphoric acid standard was introduced into the NMR tube. The NMR spectrum of the substrate was taken under these conditions. Subsequently 100 μl of the esterase solution was introduced into the NMR tube, the contents were carefully shaken for a minute. The spectrum was then taken and periodically monitored to ascertain the disappearance of the starting material.

5.4. General method for the enzymatic reactions of phosphoramidate and thiophosphoramidate derivatives of d4T as monitored by HPLC

The sample was dissolved in a known quantity of aqueous methanol and was injected into the column to obtain the starting material HPLC peaks. For the enzymatic reactions, the concentration of the enzyme was kept constant at 50 μl and the substrate concentration was varied keeping the volume constant throughout the HPLC analysis. All the enzymatic reactions were conducted at room temperature. A Lichrospher analytical column was used and the conditions were set at 1 ml min^{-1} isocratic flow. The eluent used was water (0.1% TEA + 0.1% TFA)/acetonitrile (65:35). The column was maintained at room temperature. The wavelength of absorbance was set at 265 nm with a reference value of 400 nm. The injection volume was maintained at 50 μl per sample. The experiments were repeated three times.



Substituent R	X = S	X = O	Sulfur/Oxy Ratio
	Mean (nM) \pm SEM (N=3)	Mean (nM) \pm SEM (N=3)	
4-Br	3635.3 \pm 3527.3	1.0 \pm 0.0	3635
4-OMe	8177.7 \pm 7646.2	2.7 \pm 1.7	3067
H	2613.7 \pm 2233.8	1.7 \pm 0.7	1568
4-F	997.7 \pm 726.4	1.0 \pm 0.0	998

Fig. 11. Anti-HIV activity of aryl phosphoramidate and aryl thiophosphoramidate derivatives of **1**. IC_{50} values (HIV virus) were compared for similarly substituted groups (4-Br, 4-OMe, H, 4-F) on the phenyl ring on thiophosphoramidates (horizontal line pattern) and phosphoramidates (diamond pattern) compounds. The table shows the mean and standard error calculated for each group of compounds (N replicates) and the relative potency. All thiophosphoramidate compounds showed much reduced activity with IC_{50} values >900-fold as compared to phosphoramidate derivatives.

5.5. Calculation of the rate of reaction

The rate of reaction was computed by using first order rate constants and an average of eight to nine time points were used for this estimate. Energy of activation values for individual products was obtained using the standard Arrhenius equation. The rate constants were obtained for each of the products at various temperatures and plotted and expressed in kcal mol^{-1} . The rate constants refer to rate per h since some of the reactions were too slow even at high temperatures.

We used the ANCOVA to study the influence of a categorical predictor variable (chemical substitution group) and a continuous predictor variable (Hammett sigma values) on a response variable (E_a values/ $T\Delta S$). In this analysis, the variance explained by the categorical and the continuous variables can be compared. Also, a significant effect of the categorical variable can be assigned taking into account the relationship between the continuous variable and the response variable. ANCOVA model was used to test for significant effects of Hammett sigma or $X = S/X = O$ groups on the

molecule. In this analysis the effect of the categorical variables ($X = S/X = O$ groups) were compared controlling for Hammett sigma values as the covariate. The amount of variance explained by Hammett sigma and the groups were deemed significant if the P -values were less than 0.05. Regression analysis was performed to investigate the effect of Hammett sigma on the energy of activation (E_a) and entropy ($T\Delta S$) for substrate disappearance. The amount of variance explained by Hammett sigma was expressed as R^2 values.

5.6. In vitro assays of anti-HIV-1 activity

Normal human peripheral blood mononuclear cells (PB-MNC) from HIV-negative donors were cultured for 72 h in RPMI 1640 supplemented with 20% (v/v) heat-inactivated fetal bovine serum (FBS), 3% interleukin-2, 2 mM L-glutamine, 25 mM HEPES, 2 g l^{-1} NaHCO_3 , 50 $\mu\text{g ml}^{-1}$ gentamicin, and 4 $\mu\text{g ml}^{-1}$ phytohemagglutinin prior to exposure to HIV-1 at a multiplicity of infection (MOI) of 0.1 during a 1 h adsorption period at 37 °C in a humidified 5% CO_2 atmosphere. Subsequently, cells were cultured in 96-well microtiter plates (100 μl per well; 2×10^6 cells per ml) in the presence of various concentrations of the compounds and aliquots of culture supernatants were removed from the wells on the seventh day after infection for p24 antigen assays, as previously described [31]. The applied p24 enzyme immunoassay (EIA) was the unmodified kinetic assay commercially available from Coulter Corporation/Immunotech, Inc. (Westbrooke, ME), which utilizes a murine mAb to HIV core protein coated onto microwell strips to which the antigen present in the test culture supernatant samples binds. Percent viral inhibition was calculated by comparing the p24 values from untreated infected cells (i.e. virus controls).

References

- [1] R.H. Goldschmidt, B.J. Dong, J. Am. Board Fam. Pract 10 (1997) 144–167.
- [2] S.G. Deeks, P.A. Volberding, AIDS Clin. Rev (1997–98) 145–185.
- [3] P.M. Grob, J.C. Wu, K.A. Cohen, R.H. Ingraham, C.K. Shih, K.D. Hargrave, T.L. Mctague, V.J. Merluzzi, AIDS Res. Hum. Retrovirus 8 (1992) 145–152.
- [4] F.W. Bell, A.S. Cantrell, M. Hogberg, S.R. Jaskunas, N.G. Johansson, C.L. Jordan, M.D. Kinnick, P. Lind, J.M. Morin Jr, R. Noreen, B. Oberg, J.A. Palkowitz, C.A. Parrish, P. Pranc, C. Sahlberg, R.T. Ternansky, R.T. Vasileff, L. Vrang, S.J. West, H. Zhang, X.X. Zhou, J. Med. Chem 38 (1995) 4929–4936.
- [5] A.S. Cantrell, P. Engelhardt, M. Hogberg, S.R. Jaskunas, N.G. Johansson, C.L. Jordan, J. Kangasmetsa, M.D. Kinnick, P. Lind, J.M. Morin Jr, M.A. Muesing, R. Noreen, B. Oberg, P. Pranc, C. Sahlberg, R.J. Ternansky, R.T. Vasileff, L. Vrang, S.J. West, H. Zhang, J. Med. Chem 39 (1996) 4261–4274.
- [6] R. Vig, T.K. Venkatachalam, F.M. Uckun, Antiviral Chem. Chemother 9 (1998) 445–448.
- [7] C. Mao, R. Vig, T.K. Venkatachalam, E.A. Sudbeck, F.M. Uckun, Bioorg. Med. Chem. Lett 8 (1998) 2213–2218.
- [8] P.A. Furman, J.A. Fyfe, M.H. St. Clair, K. Weinhold, J.L. Rideout, G.A. Freeman, L.S. Nusinoff, D.P. Bolognesi, S. Broder, H. Mitsuya, D.W. Barry, Proc. Natl. Acad. Sci. USA 83 (1986) 8333–8337.

- [9] Z. Hao, D.A. Cooney, N.R. Hartman, C.F. Perno, A. Fridland, A.L. De Vico, M.G. Sarngadharan, S. Border, D.G. Johns, *Mol. Pharmacol* 34 (1988) 431–435.
- [10] J. Balzarini, D.A. Cooney, M. Dalal, G.J. Kang, J.E. Cupp, E. De Clercq, S. Broder, D.G. Johns, *Mol. Pharmacol* 32 (1987) 798–806.
- [11] C. McGuigan, D. Cahard, H.M. Sheeka, E. De Clercq, J. Balzarini, *J. Med. Chem* 39 (1996) 1748–1753.
- [12] C. McGuigan, D. Cahard, H.M. Sheeka, E. De Clercq, J. Balzarini, *Bioorg. Med. Chem. Lett* 6 (1996) 1183–1186.
- [13] M.G. Starnes, Y.C. Cheng, *J. Biol. Chem* 262 (1987) 988–991.
- [14] Z. Hao, D.A. Cooney, D. Farquhar, C.F. Perno, K. Zhang, R. Masood, Y. Wilson, N.R. Hartman, J. Balzarini, D.G. Johns, *Mol. Pharmacol* 37 (1990) 157–163.
- [15] M.A. Johnson, G. Ahluwalia, M.C. Connelly, D.A. Cooney, S. Broder, D.G. Johns, A. Fridland, *J. Biol. Chem* 263 (1988) 15354–15357.
- [16] M.A. Johnson, A. Fridland, *Mol. Pharmacol* 36 (1989) 291–295.
- [17] C. McGuigan, R.N. Pathirana, J. Balzarini, E. De Clercq, *J. Med. Chem* 36 (1993) 1048–1052.
- [18] C. McGuigan, R.N. Pathirana, N. Mahmood, K.G. Devine, A. Hay, *J. Antiviral Res* 17 (1992) 311–321.
- [19] R. Vig, C. Mao, T.K. Venkatachalam, L. Tuel-Ahlgren, E.A. Sudbeck, F.M. Uckun, *Bioorg. Med. Chem* 6 (1998) 1789–1797.
- [20] T.K. Venkatachalam, T.L. Tai, R. Vig, C.L. Chen, S.T. Jan, F.M. Uckun, *Bioorg. Med. Chem. Lett* 8 (1998) 3121–3126.
- [21] F.M. Uckun, P. Samuel, S. Qazi, C.L. Chen, S. Pendergrass, T.K. Venkatachalam, *Antiviral Chem. Chemother* 13 (2002) 197–203.
- [22] C.L. Chen, G. Yu, T.K. Venkatachalam, F.M. Uckun, *Drug Metab. Dispos* 30 (2002) 1523–1531.
- [23] R. Lohrmann, L.E. Orgel, *J. Mol. Evol* 7 (1976) 253–267.
- [24] M. Oivanen, S. Kuusela, H. Lonnberg, *Chem. Rev* 98 (1998) 961–990.
- [25] S. Mikkola, M. Kosonen, H. Lonnberg, *Curr. Org. Chem* 6 (2002) 523–538.
- [26] P. Jarvinen, M. Oivanen, H. Lonnberg, *J. Org. Chem* 56 (1991) 5396–5401.
- [27] M. Ora, K. Mattila, T. Lonnberg, M. Oivanen, *J. Am. Chem. Soc* 124 (2002) 14364–14372.
- [28] N. Mesplet, Y. Saito, P. Morin, L.A. Agrofoglio, *Bioorg. Chem* 31 (2003) 237–247.
- [29] J. March (Ed.), *Advanced Organic Chemistry*, Wiley, New York, 1992.
- [30] J.D. Annette, *Texts in Statistical Science: An Introduction to Generalized Linear Models*, second ed, Chapman and Hall/CRC. A CRC Press Company, Boca Raton, London, New York, Washington, DC, 2002.
- [31] F.M. Uckun, L.M. Chelstrom, L. Tuel-Ahlgren, I. Dibirdik, J.D. Irvin, M. Chandan-Langlie, D.E. Myers, *Antimicrob. Agents Chemother* 42 (1998) 383–388.